RAMAN MICRO-SPECTROSCOPY MAPPING AND MICROSTRUCTURAL AND MICROMECHANICAL STUDY OF INTERFACIAL TRANSITION ZONE IN CONCRETE REINFORCED BY POLY(ETHYLENE TEREPHTHALATE) FIBRES

VLADIMÍR MACHOVIČ*, ***, LUBOMÍR KOPECKÝ*, JIŘÍ NĚMEČEK*, FRANTIŠEK KOLÁŘ***, JAROSLAVA SVÍTILOVÁ***, ZDENĚK BITTNAR**, JANA ANDERTOVÁ*

*Institute of Chemical Technology Prague, Technická 5, 166 28, Prague, Czech Republic
**Faculty of Civil Engineering, Czech Technical University in Prague, Thakurova 7, 166 29 Prague, Czech Republic
***Institute of Rock Mechanic and Structure AS CR, V Holešovičkách 41, 182 09 Prague, Czech Republic

E-mail: vladimir.machovic@vscht.cz

Submitted October 4, 2007; accepted January 9, 2008

Keywords: Interfacial transition zone, Raman spectroscopy, Microstructure, PET fiber reinforcement

A new application, the Raman microspectroscopy mapping technique, was successfully used to study of the interfacial transition zone (ITZ) around poly(ethylene terephtalate) (PET) reinforcement in concrete. Waste from PET bottles has been used in form of fibers as a reinforcing element in Portland cement concrete. Raman spectra represent the compositional variation of the cement matrix within the distance range of 5 to 65 μm from the PET fibre. The Raman band at 357 cm^{-1} corresponding to the vibrations of Ca–O bond at $Ca(OH)_2$ was used for quantitative distribution of portlandite within the ITZ area. The most intensive band of portlandite occurs at the distance from 0 to 30 μm from the PET fibre. Raman spectroscopy has been completed with nanoindentation and environmental scanning electron microscopy (ESEM) in combination with microanalysis (EDX), and electron diffraction (EBSD-OIM). The contact zone is characterized by a higher porosity (both air and water pores) and occurrence of newly formed mineral phases - portlandite, hydrocarbonate, ettringite, and lower Ca^{2+} saturated C–S–H gels.

INTRODUCTION

The concrete is considered as a three-phase composite, including cement matrix, aggregate, and interfacial transition zone (ITZ). The first works on the ITZ were published in 1950s by Farran [1,2]. It is well known that the ITZ between aggregate/fibre and matrix is microstructurally different from the bulk cement paste, and the fibre-matrix bond properties are critical in determining the concrete properties. In the case of special reinforcing materials (e.g. pulp fibres, asbestos, etc.) the ITZ cannot be observed. The origin of the ITZ consists in the so called "wall effect" of packing of small cement grains around each aggregate particle. Therefore, porosity and the water-to-cement (w/c) ratio increase from the bulk cement paste to the surface of aggregate particles. According to numerous studies, the thickness of the ITZ is 15-50 μm. The typical thickness of the transition zone between a aggregate/fibre and bulk cement paste is approximately 50 μm. The adhesion between aggregate and cement paste within the transition zone is a factor that controls the concrete strength. The transition zone is considerable weaker than the bulk matrix due to large calcium hydroxide crystals and needle-shaped ettringite in the open pores within the ITZ as shown by microhardness tests. This weak phase may be diminished by silica fume or superplasticizer controlling packing density and hydration around aggregate surface [3].

Studies on the microstructure and composition of the cement paste near the ITZ have been made by means of environmental scanning electron microscopy (ESEM) and porosimetry analysis. Recently, FT-IR and Raman spectroscopies have been successfully utilized to study concrete hydration products. On the other hand, research that has applied Raman spectroscopy to the concrete ITZ analysis has been rarely reported [4].

A growing volume of PET waste produced by modern society is a worldwide problem. PET has succeeded as a consumer-friendly material for beverage bottles. The worldwide production of PET for packing is about 13.106 t/year [5]. Therefore re-utilization of PET waste is of considerable ecological importance. Different PET fiber types with various properties can be used for

cement reinforcement [6-7]. In general, fibers made of a high-strength, high-modulus material, such as glass, carbon, etc., will usually increase the strength and toughness of the cement composite. In case of low-modulus material, such as polypropylene and polyethylene, the reinforcement enhance mainly the ductility of the cement composite, but not its strength, resulting in strain softening or elastic-plastic behavior [8]. Several researchers studied the influence of the modulus of elasticity of the fibers on the bond between the fiber and the cement matrix [9-10]. As shown in the studies, increasing modulus of elasticity of the fiber enhances the bond strength.

In this paper, the Raman microspectroscopy mapping technique was used to study the interfacial transition zone (ITZ) around monofilament poly(ethylene terephtalate) (PET) fibre in reinforced concrete. Raman spectroscopy has been completed with nanoindentation and ESEM in combination with microanalysis, and electron diffraction. The aim of the study is to describe the specific properties of the ITZ between PET fibers and bulk cement matrix as a substantial area for prediction of mechanical behavior of large scale bodies.

EXPERIMENTAL

Sample preparation

Sample was prepared by mixing 200 g of Portland cement (chemical properties are shown in table 1), 100 g of water, 140 g of sand of granular fraction 1.5-2.5 mm, 12 g of sand of granular fraction 0.5-1 mm, and 20 g of stone fragments. PET fibers were used as reinforcing components at mass volume of 2 wt %. The fibers are produced in a factory (Silon, Planá nad Lužnicí, Czech Republic) that recycles PET bottles. The fibers were added to the concrete mixtures as monofilaments with a diameter of 200 μm and length of about 10 mm. After hydration for 180 days, hardened samples were sawed and their surface brushed and polished, which is the crucial phase of the preparation procedure. Each element of a composite material like PET has different response to the mechanical stress. Standard methods of polishing are not suitable. Instead, after the fine cutting, we used sanding the sample with the finest papers (SiC 2000, SIA 8) for 1 minute only, followed by polishing with a diamond paste for 1.5 hour. Also, the planned experiments required to stop the hydration processes in the cement matrix. Ethanol is a suitable agent for stopping the evolution of carbonates at the surface of the cement paste. For the next experimental procedures the fibers in different orientation with respect to the cross-section have been chosen. Best results have been obtained from both the parallel and exact perpendicular oriented section.

Instrumentation

Raman spectra were collected using the LabRam system Jobin Yvon, model Labram HR, equipped with a 532 nm line laser for excitation of cement materials. The laser power and the time of sample excitation were adjusted to obtain high quality Raman spectra, enabling creation of spectral maps. The scattered light was analyzed by a spectrograph with holographic grating (600 gr/mm), slit width of 100 μm, and opened confocal hole (1000 μm). Adjustment of the system was regularly checked using a silicon sample (520.5 cm^{-1}) and by measurement in the zero-order position of the grating. The acquisition time for a particular spectral window was 15 s. Ten accumulations were co-added to obtain a spectrum. The five micron step was selected for microspectroscopic mapping and whole mapping area was 30×75 μm. The average spectrum was computed from six of the measured mapped spectra. Figure 1 shows the schematic diagram of the LabRam system.

Micromechanical properties of ITZ in a cementitious matrix can be effectively studied by means of nanoindentation. This technique is based on the direct measurement of the load-displacement relationship using a very sharp diamond tip pressed into a material. The Nanotest nanoindenter by Micromaterials, UK

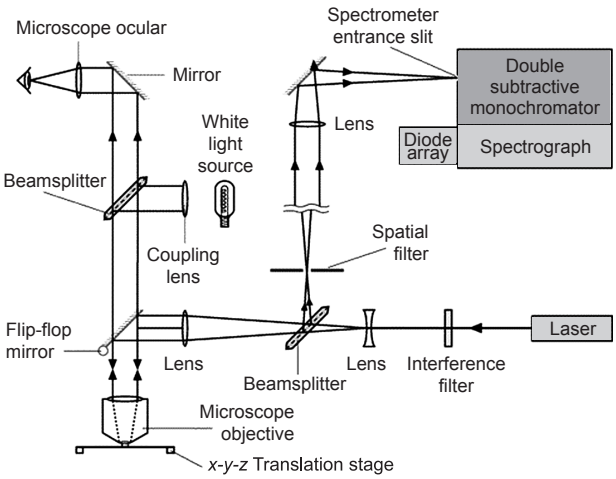

Figure 1. Schematic diagram of the LabRam system.

Table 1. Chemical properties of cement.

Chemical analysis (%)	SiO_2	Al_2O_3	Fe_2O_3	CaO	MgO	SO_3	Na_2O	K_2O
cement	25.93	11.76	2.35	51.18	1.04	4.29	0.62	1.17

equipped with a standard Berkowich tip was used for all measurements. In order to capture properties of the transition zone and due to the large heterogeneity of the matrix, it was necessary to perform multiple indents in the PET fibre neighborhood. Eight rows and twelve columns of indents were produced to the maximum load of 12 mN that corresponded to the maximum indentation depth of about 1μm in cementitious matrix. The distance of individual indents was 10 μm and the total area covered by indentation was 80×120 μm. It was unavoidable to produce indents in all material phases including clinkers and/or aggregate grains. Therefore indents were subsequently separated into individual groups by ESEM/EDX measurements. Only results for a fully hydrated cement paste (i.e. C–S–H and portlandite phase) were considered in the evaluation. Elastic properties of this phase were evaluated according to a standard procedure from unloading branches of the indentation curves. The scatter of results given by the different composition of indented places was captured by statistical evaluation of results from individual columns corresponding to individual distances from a PET fibre.

The environmental scanning electron microscope - XL30 ESEM FEI PHILIPS - was equipped with a set of electron detectors: SED (GSED) for micromorphology, and BSED (GBSED) for phase contrast both in the high vacuum and environmental modes. The EDX analysis of secondary X-ray spectra provides the quantitative chemical composition of selected objects (particles), maps of the element distribution, and quantitative profiles. The mineral composition at the microlevel was facilitated by newly installed OIM-EBSD (Orientational Imaging Microscopy - Electron Back Scattered Diffraction). The OIM method is based on the same laws (Bragg's laws) as X-ray diffraction. The system is equipped with a large library of diffraction data and gives quantitative information about mineral composition.

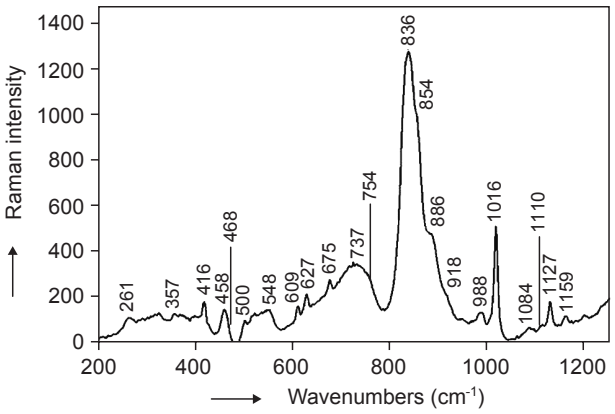

Figure 2. Raman spectrum of the original Portland cement.

With respect to the time consuming experimental procedures only five micromechanical sets on five polished section have been carried out.

RESULTS AND DISCUSSION

The cement hydration process can be represented by a set of chemical equations that describes the hydration of the main cement mineral phases C_3S, C_2S, C_3A, and C_4AF (the nomenclature used here for cement is C = CaO, S = SiO_2, H = OH, A = Al_2O_3, F = Fe_2O_3, S = SO_4). In the cement chemistry, Raman spectroscopic analysis has traditionally been a laboratory tool for structural analysis of cement clinkers and hydration products. Recent developments in instrumentation, however, make it possible to use Raman spectroscopy as a tool for identification of minerals distribution by microspectroscopy mapping. Figure 2 shows average Raman spectrum of the original Portland cement, which has been computed from fifteen of the mapped spectra obtained with 50× magnification objective. Spectral manipulation such as baseline adjustment and minor smoothing was performed. The stretching vibration bands of Si–O characteristics of C_3S and β-C_2S phases can be seen in the Raman spectrum in the 800-900 cm^{-1} region. The most intensive band at 836 cm^{-1} has been assigned to C_3S, and the band at 854 cm^{-1} to C_2S/C_3S. A shoulder at 886 cm^{-1} can be assigned to satellites of alite and belite. The bands in the region between 525 to 550 cm^{-1} have been assigned to O–Si–O bending modes of C_3S/C_2S [11]. Broad feature near 730 cm^{-1} is composed of vibration of C4AF at 737 cm^{-1} and of C_3A at 754 cm^{-1} [12]. The bands at 416, 492, 675. 1016, and 1159 cm^{-1} can be assigned to the bassanite ($CaSO_4 \cdot 0.5 H_2O$) modes. The weak band at 1084 cm^{-1} is due to C–O stretching in the carbonate groups present in calcium carbonate. The bands at the 200-400 cm^{-1} region probably belong to Ca–O vibrations [12, 13].

The area of interest in the vicinity of a PET fibre shows the matrix of nanoindents (see Figure 3). The distance of nanoindents applied is significantly shorter than the minimum distance acquired according to the norm EN ISO 14577-1. However, this norm has been established for metallic materials. In contrast to the compact structure of such materials, the cementitious based composite are porous, containing wide size spectrum of pores. The porosity absorbs the effect of indentation. The target area represents very intimate contact and a very well preserved ITZ between the PET fibre and the hydrated cement paste. It indicates a very good quality of the sample preparation. The same part of ITZ has been selected for Raman micro-spectroscopy mapping (see Figure 4). The dots represent the matrix of 6×15 testing points with regular distance of 5 μm.

Figure 5 shows the average Raman spectra obtained by point measurements along the matrix (see Figure 4). The spectra represent the compositional variation of the cement matrix within the distance range of 5-65 μm from a PET fibre with a step of 5 μm.

After 180 days of hydration, prominent changes clearly take place in the region between 200 and 1200 cm^{-1} in the Raman spectra of the cement matrix depending on the distance from the PET filament. The intensities indicating starting occurence of clinker minerals diminished or even disappeared entirely. The band of alite (C_3S) at 836 cm^{-1} does not occur in the spectra of hydrated cement, whereas the presence of the belite (C_2S) band at 858 cm^{-1} can not be evaluated due to a coincidence with the PET band at 857 cm^{-1} (see Figure 5). The content of belite increases with the distance from the PET fibre. There are no bands near 730 cm^{-1} in the spectra that confirms complete hydration of the C_3A and C_4AF phases. The intensity of a band near 540 cm^{-1} increases with increasing distance from the PET fiber. The band is probably attributed to the presence of an unhydrated clinker [12].

The increasing intensities of CH, C–S–H, and ettringite bands are obvious. The dominating band at 357 cm^{-1} in Figure 5 corresponds to the vibrations of O–H bond at $Ca(OH)_2$ (portlandite). The Raman spectrum of CH shows three bands, two sharp bands at 253 and 356 cm^{-1}, and a broad band located at about 680 cm^{-1}. There is another prominent band of stretching O–H vibration at 3618 cm^{-1} (spectrum is not shown). The most intensive band of portlandite occurs at the distance from 5-30 μm from the PET fibre. The intensity of the spectrum decreases strongly with the distance. There is a lower intensity of O–H band in the region between 0-5 μm caused probably by hydrophobity of the fiber. The spectrum of C–S–H shows a broad symmetric stretching motion of the Si–O–Si mode near 660 cm^{-1}, due to the poor crystallinity of C–S–H. [12]. The intensity of the band rises with increasing distance from the fibre. The trend of the volume of calcium carbonate (with the band of CO_3 at 1080 cm^{-1}) is similar.

Raman microspectroscopy was used as a powerful technique for the analysis of ettringite ($C_6A\ S_3H_{32}$) in hydrated cement. The intensity of the ettringite υ_1 [SO_4] and υ_3 [SO_4] bands at 988 cm^{-1} and 1130 cm^{-1}, respec-

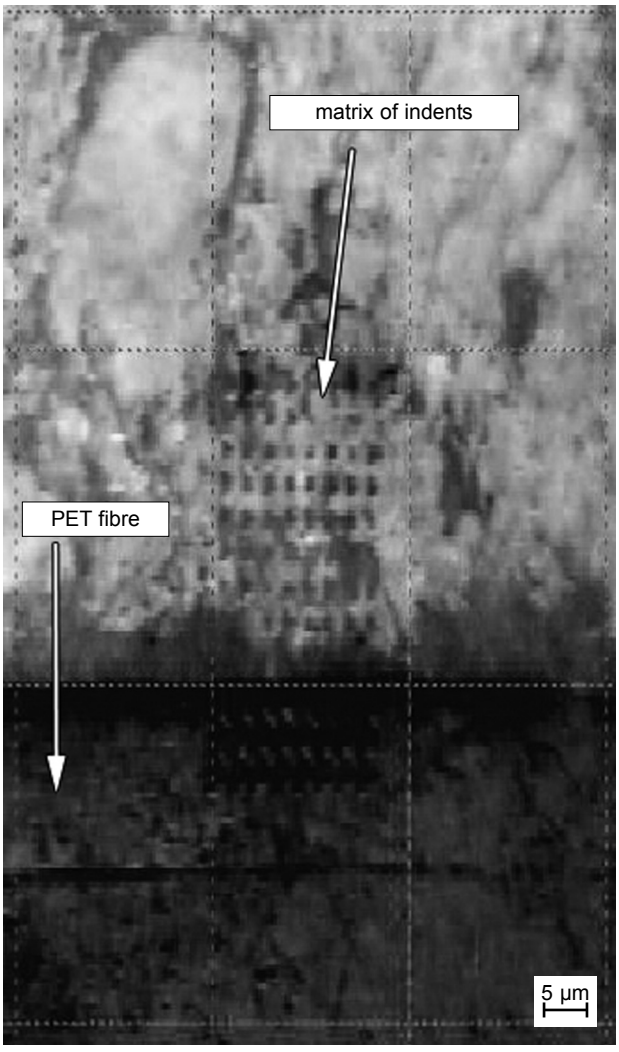

Figure 3. Micrograph of a PET fibre in the cement paste with the matrix of nanoindents.

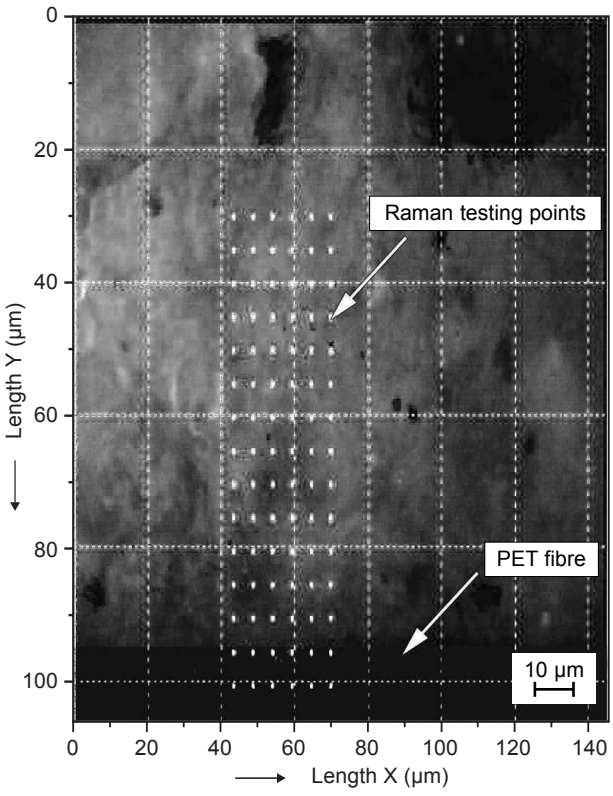

Figure 4. Micrograph of the cement paste reinforced by a PET fibre (the dark band at the bottom part) with the matrix (6×15 testing points) of Raman spectra.

tively, increase as well with the distance from the PET filament. The band of alite (C_3S) occurs in the spectrum at 858 cm^{-1}. The volume of alite increases with the distance from the PET fibre. The band in the 1050-1100 cm^{-1} region can be assigned to symmetrical C–O stretching vibrations of carbonate different forms generated mainly by carbonation of calcium hydroxide. The two sharp bands at 789 and 968 cm^{-1} observed in a single case are due to SiC contamination from sanding the sample. The bands at 634, 1001 and 1093 cm^{-1} are due to spectral crosscontamination from the PET fibre.

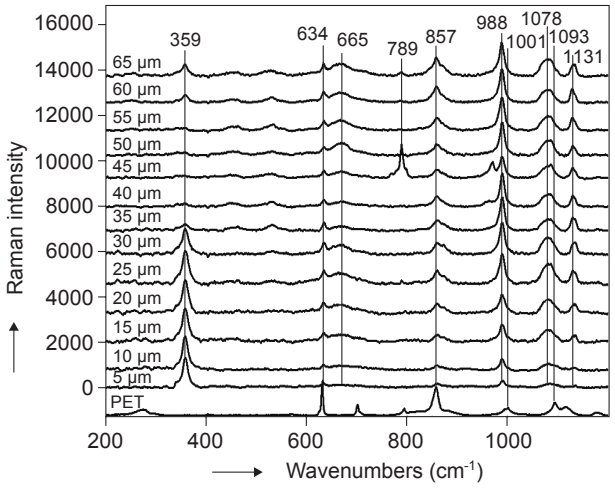

Figure 5. Plot of the average Raman spectra of the cementitious matrix - the step of testing points is 5 µm from the PET fibre.

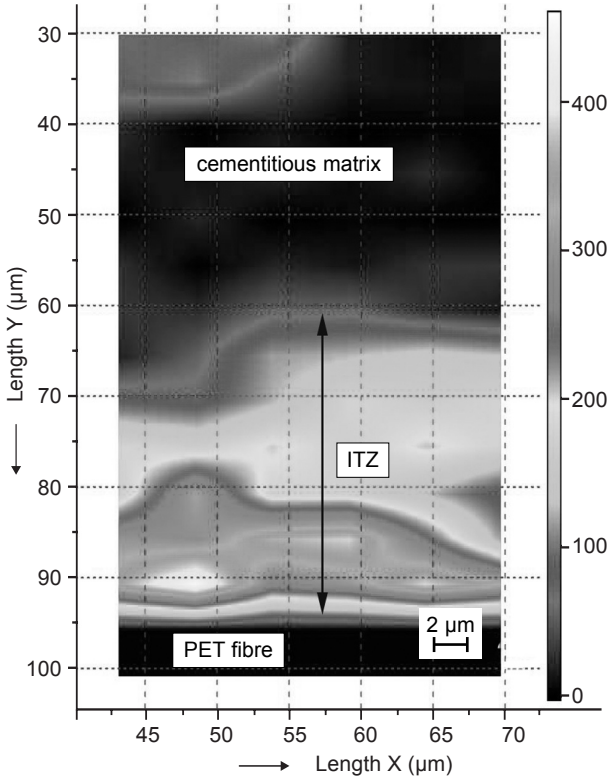

Figure 6. Map of occurrence of portlandite at 357 cm^{-1} in the cementitious matrix.

The synoptical arrangement of the Raman intensity mapping for the band of portlandite at 357 cm^{-1} in the cement matrix is plotted in Figure 6. The richest area of the calcium hydroxide evolution within ITZ occurs at 2.5-20 µm from the fibre. The width of the portlandite rich zone is irregular - it is reduced to 5 µm only on the other side of the map. The occurence of portladite varies at the band within 30 µm. The similar map can be seen for portlandite stretching O–H band at 3618 cm^{-1}.

Results of elastic modulus have been evaluated as the mean values dependent on the distance from the PET fibre (see Figure 7). The first three values correspond to the elastic modulus of PET itself. The subsequent indents were produced in ITZ and the bulk of cementitious matrix. It is clearly evident that the width of ITZ is about 40 µm around the fibre. The rest of indents lies in the bulk not affected by the fibre. The scatter of results given by standard deviations is typical for cementitious materials and is given by its heterogeneity.

Microstructure, phase composition and chemistry of the ITZ in cementitious matrix studied by means of ESEM/EDX/EBSD are illustrated by micrographs taken in secondary electrons (SE) and in backscattered electrons (BSE), presented in Figure 8a and 8b, respectively. The discrimination and phase identification of C–S–H and other particles in the target area of indents has been done according to both BSE images as well as EDX. The microstructure of the cement paste is different if compared with the bulk cement matrix away from the interface. The micronalyses reveal the zonal composition of the microstructure, i.e. the concentric radial texture in relation to the fibre, and the zonal mineralogical and chemical composition of newly formed cementitious phases in the ITZ around the fibres.

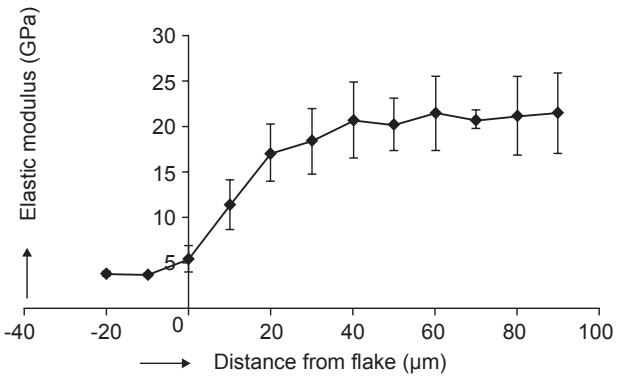

Figure 7. The evolution of elastic modulus E [GPa] from a PET fibre to cementitious matrix (ITZ can be clearly distinguished within the first 40 µm from the fibre).

The ITZ is characterized by a porous structure on microlevel formed by two types of pores: circular shaped pores filled with dragged air of a diameter of tenths of μm, and irregularly shaped pores filled with seggregated water rich in Ca^{2+} ions. These are often filled with aggregates of fine microcrystals of portlandite and/or ettringite.

In the chemical composition of ITZ, portlandite and the low Ca saturated C–S–H phases prevail. The fully Ca-saturated (i.e., C_3–S–H) clusters are present in the bulk paste only. Very good correlation between the spatial distribution of selected components correlates very well with the E-modulus. The near contact zone of ITZ, i.e., the first 10.0 microns, is characterized by lower E-modulus values, varying from 5.0 to 10.0 GPa, lack of fully Ca-saturated C–S–H gels, and a high volume of portlandite and $Ca(HCO_3)_2$. This is a consequence of higher porosity caused by the partially hydrophobic surface of PET (see Figure 8). For utilization of the recycled PET fibers for cement reinforcement, it would be desirable to modify their surface activity by chemical agents in order to improve the interfacial adhesion between the fiber and cementitious matrix.

CONCLUSION

A new application of the Raman microspectroscopy mapping technique and nanoindentation, ESEM/EDX/ /EBSD-OIM analyses to the investigation of the interfacial transition zone (ITZ) as a cross-over element between poly(ethylene terephtalate) (PET) reinforcement and concrete mass has been presented. ITZ has been characterized by following features:

- The width of ITZ in PET reinforced concretes varies from 20 to 40 μm. This statement has been based on micromechanical properties, on chemical variability in composition of cement paste, on mineralogy, and on structural arrangement of freshly formed mineral phases.

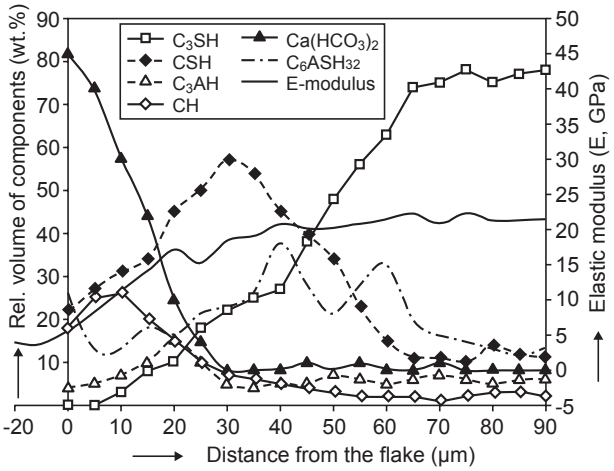

Figure 9. The variations in mineral composition, C–S–H gels volume, Ca^{2+} saturation of C–S–H gels, and E-modulus, as a function of a distance from a PET fibre.

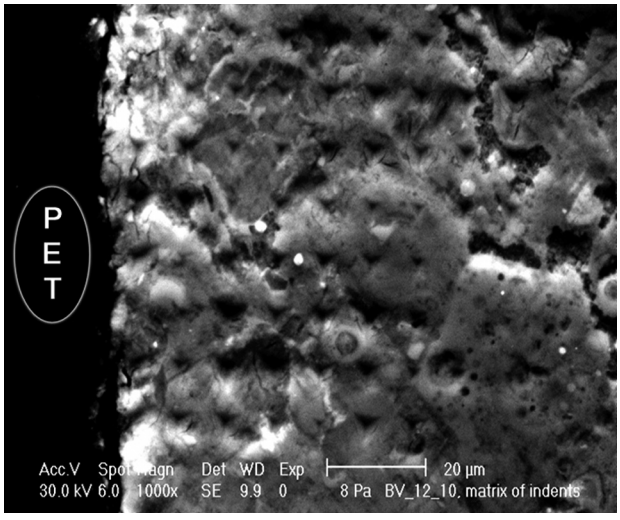

a)

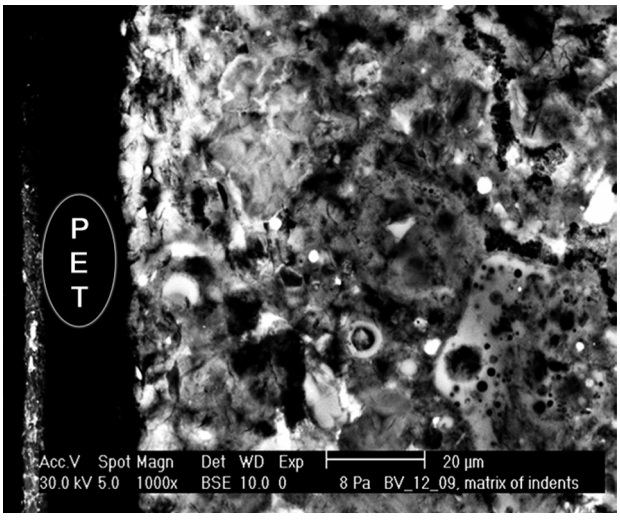

b)

Figure 8. Micrographs of the ITZ with the area of the matrix of indents. The left picture (a) taken in SE shows the morphology of the surface. The right picture (b) taken in BSE shows the phase contrast. The white particles are the rests of unhydrated clinkers or $Ca(HCO_3)_2$ in the case of intimate contact with the fibre. The pale gray areas represent the islets rich in portlandite. The most hydrated parts of the cementitious matrix rich in C_3SH gels are dark gray. The edge of the PET fibre (black) is at the left side of both micrographs.

- The structural, mineralogical and chemical variability in the phase and mineral composition of ITZ is zonal with radial arrangement of the mineral phases (ettringite, Ca-carbonates) formed freshly at the boundary.
- The specific feature of ITZ is increasing volume of porosity in contrast to bulk concrete. The porosity seems to be partially caused by hydrophobic behavior of the PET surface. Two types of pores (water and air) have been distinguished. Water pores of an irregular shape are filled with portlandite, ettringite and calcite formed freshly from segregated water rich in Ca^{2+} ions. They are formed in micro-shear zones of the material. The air pores have a radial shape and are filled with thin incrustation of ettringite and Ca-carbonates on their inner surfaces. The C–S–H gels of ITZ are thus lower Ca^{2+} saturated and do not form the C_3S–H gels like in the bulk paste.
- Good correlations between the spatial distribution of selected components (types of C–S–H gels, mineralogy and porosity) and E-modulus have been found.

Acknowledgement

This work has been kindly supported by Grant No. 106/05/2618 of the Grant Agency of the Czech Republic and Research plan MSM 6840770003 of the Ministry of Education of the Czech Republic.

References

1. Farran C. R.: Seances Acad.Sci.Paris *27*, 73 (1953).
2. Farran C. R.: Rev.Mater.Construct. *491*, 155 (1956).
3. Ollivier P., Maso J. C., Bourdette B.: Advn.Cem.Bas.Mat. *2*, 30 (1995).
4. Lo T. Z., Cui H. Y.: Mat.Lett. *58*, 3089 (2004).
5. Viksne A., Kalnins M., Rence L., Berzina R.: Arab.J.Sci. Eng. *27*, 33 (2002).
6. Bentur A., Midness S.: *Fibre reinforced cementious composites*, Elsevier, Amsterodam 1990.
7. Balagru P. N., Shah S. P.: *Fiber reinforced cement composites*, McGraw-Hill, New York 1992.
8. Silva D. D. A., Betioli A. M., Gleize P. J. P., Roman H. R., Gómez L. A., Ribeiro J. L. D.: Cem.Concr.Res. *35*, 1741 (2005).
9. Shang H.: Adv.Cem.Bas.Mater. *4*, 106 (1996).
10. Peled A., Bentur A.: Cem.Concr.Res. *30*, 781 (2000).
11. Potgieter-Vermaak S. S., Potgieter J. H., Belleil M., DeWeerdt F., Van Grieken R.: Cem.Concr.Res. *36*, 656, (2006).
12. Deng C.-S., Breen C., Yarwood J., Habesch S., Phipps J., Craster R., Maitland G.: J.Mat.Chem. *11*, 3105 (2002).
13. Tarrida M., Madon M., Le Rolland B., Colombet P.: Advn. Cem.Bas.Mat. *2*, 15 (1995).
14. Martinez-Ramirez S., Frías M., Domingo C.: J. Raman Spectrosc. *37*, 555 (2006).

STUDIUM PŘECHODOVÉ FAZE CEMENTOVÉHO KOMPOZITU VYZTUŽENÉHO PET VLÁKNY POMOCÍ MAPOVÁNÍ RAMANOVOU SPEKTROSKOPIÍ, MIKROSTRUKTURNÍ A MIKROMECHANICKÉ ZMĚNY

VLADIMÍR MACHOVIČ*.***, LUBOMÍR KOPECKÝ*, JIŘÍ NĚMEČEK*, FRANTIŠEK KOLÁŘ***, JAROSLAVA SVÍTILOVÁ***, ZDENĚK BITTNAR**, JANA ANDERTOVÁ*

**Ústav skla a keramiky, Vysoká škola chemicko-technologická, Technická 5, 166 28, Praha 6*
***Fakulta stavební, České vysoké učení technické, Thákurova 7, 166 29 Praha 6*
****Ústav struktury a mechaniky hornin AVČR, v.v.i, V Holešovičkách 41, 182 09 Praha 8*

Pro studium přechodové zóny mezi PET vláknem a cementovou matricí bylo s úspěchem použito mapování Ramanovou spektroskopií. Jako mikrovýztuž byla použita vlákna vyrobená z odpadních PET lahví a jako matrice byl použit portlandský cement. Ramanovou spektroskopií byly sledovány strukturní změny cementové matrice ve vzdálenosti 5-65 μm od PET vlákna. Pás při 357 cm^{-1} odpovídající vibraci Ca–O vazby v $Ca(OH)_2$ byl použit pro stanovení jeho kvantitativní distribuce v přechodové zóně. Nejintenzivnější pásy portlanditu se vyskytovaly ve vzdálenosti 0-30 μm od PET vlákna. Výsledky Ramanovy spektroskopie byly doplněny výsledky elektronové mikroskopie (ESEM) v kombinaci s mikroanalýzou (EDX) a elektronovou difrakcí (EBSD-OIM). Kontaktní zóna vykazovala vyšší porozitu a výskyt nově vzniklých minerálních fází - portlandit, hydrouhličitan, ettringit a C–S–H gely.